Mineralogical Attenuation Processes Associated With The Evolution Of Acid Mine Drainage In Sulfide-Rich Mine Wastes

Teresa Valente[1], Patricia Gomes[1], Maria Amália Sequeira Braga[1], Jorge Pamplona[1];, Isabel Margarida Antunes[1], Carlos Alberto Ríos Reyes[2], Filipa Moreno[1]

[1]ICT, Institute of Earth Sciences, Pole of the University of Minho, Earth Sciences Department, Campus de Gualtar, 4710 Braga, Portugal, teresav@dct.uminho.pt; imantunes@dct.uminho.pt;masbraga@dct.uminho.pt, filipa_moreno@hotmail.com

[2]School of Geology, Universidad Industrial de Santander, Colombia, carios@uis.edu.co

Abstract

The geochemical evolution of acid mine drainage results in secondary minerals that play a key role in the environmental behavior of the mine wastes. The present work is focused on these newly formed minerals at the Penedono waste dump, characterized by fine grained tails with pyrite and arsenopyrite. Mineralogical study led to an inventory of secondary phases, comprising soluble sulfates, scorodite, and oxyhydroxysulfates. In addition, there is amorphous Fe, As rich-nanoprecipitates. Jarosite and scorodite are abundant minerals, acting as cement for encrusting tails in Fe and As-rich hardpans. These hard structures are relatively insoluble, retaining toxic elements, thereby contributing to natural attenuation of mining contamination associated with the sulphide wastes.

Keywords: Mineralogical control, scorodite, jarosite, salt efflorescences, hardpans

Introduction

Abandoned mines are important focus of environmental impact in regions with substantial mining tradition, like the North of Portugal. In sulfide-rich waste dumps acid mine drainage (AMD) may contribute to the mobility of potentially toxic elements (PTE), being responsible for water, soil and sediment contamination, sometimes over a great distance from the mines. The present study was focused in a sulfide-rich waste dump in the North of Portugal (Penedono mine) (Figure 1). This mine has been exploited for gold and arsenic until the 1990s. Presently, it is abandoned, even though the waste dumps do remain without environmental rehabilitation.

There are several works reporting the occurrence of high levels of PTE in the surrounding soils (Abreu et al. 2007). Nevertheless, some authors show the progressive colonization of the waste dumps by autochthonous species (Gomes et al. 2014), which reveals that natural attenuation processes are underway. Geochemical and mineralogical evolution lead to new mineral phases as documented in other former mining sites (e.g. Hammarstrom et al. 2005; Dold 2014; Olías and Nieto 2015; Valente et al. 2013). Therefore, the main objective of the present work relies in the identification of the secondary minerals and aggregates associated with AMD in the Penedono waste dumps. Moreover, it intends to characterize these materials, including Fe and As-rich hardpans, in order to evaluate their role in the retention of PTE and, thus, their contribution for natural attenuation processes.

Study site

Penedono was a gold and arsenic mine, located in the Northeast of Portugal. Exploitation occurred in hydrothermal deposit with quartz veins with sulfides (Figure 1). The mine wastes have abundant fine particles of quartz and arsenopyrite. Nowadays, the waste dumps present signs of strong instability enhanced by steepness and high gradient slopes. A big ravine with NE-SW orientation contributes to spatial dispersion of the mine wastes (Figure 2).

The study area is characterized by dry summers and cold winters, with average annual precipitation and temperature of

about 1700 mm/year and 21°C, respectively (IPMA, unpublished data). However, between June and September it is possible to register air temperatures higher than 30°C. A wide range of microenvironments was recorded at the waste dumps, with the temperature and humidity varied between 25-40°C and 30-70%, respectively.

Methods

Sampling included collection of surface water, salt efflorescences and hardpans in the dry season (June) of two consecutive years. The last were randomly collected to cover diverse terrain settings. Also, sampling tried to represent the macroscopic variety observed in the field, based on colors and occurrence modes. Efflorescent salts were stored in closed vessels. Humidity and temperature were measured at sampling sites with a portable hygrometer.

The mineralogical study was performed by x-ray diffraction (XRD) with CuKα radiation at 40 kV and 30 mA. Identification and paragenetic study were completed by field emission scanning electron microscopy (FESEM) after coating samples with chromium film. Hardpans were gently milled and wet sieved to < 20 μm. Diluted suspensions of this fraction were studied by transmission electron microscopy (TEM).

Water was collected at the sampling sites represented in figure 1. The background hydrochemistry was characterized by the

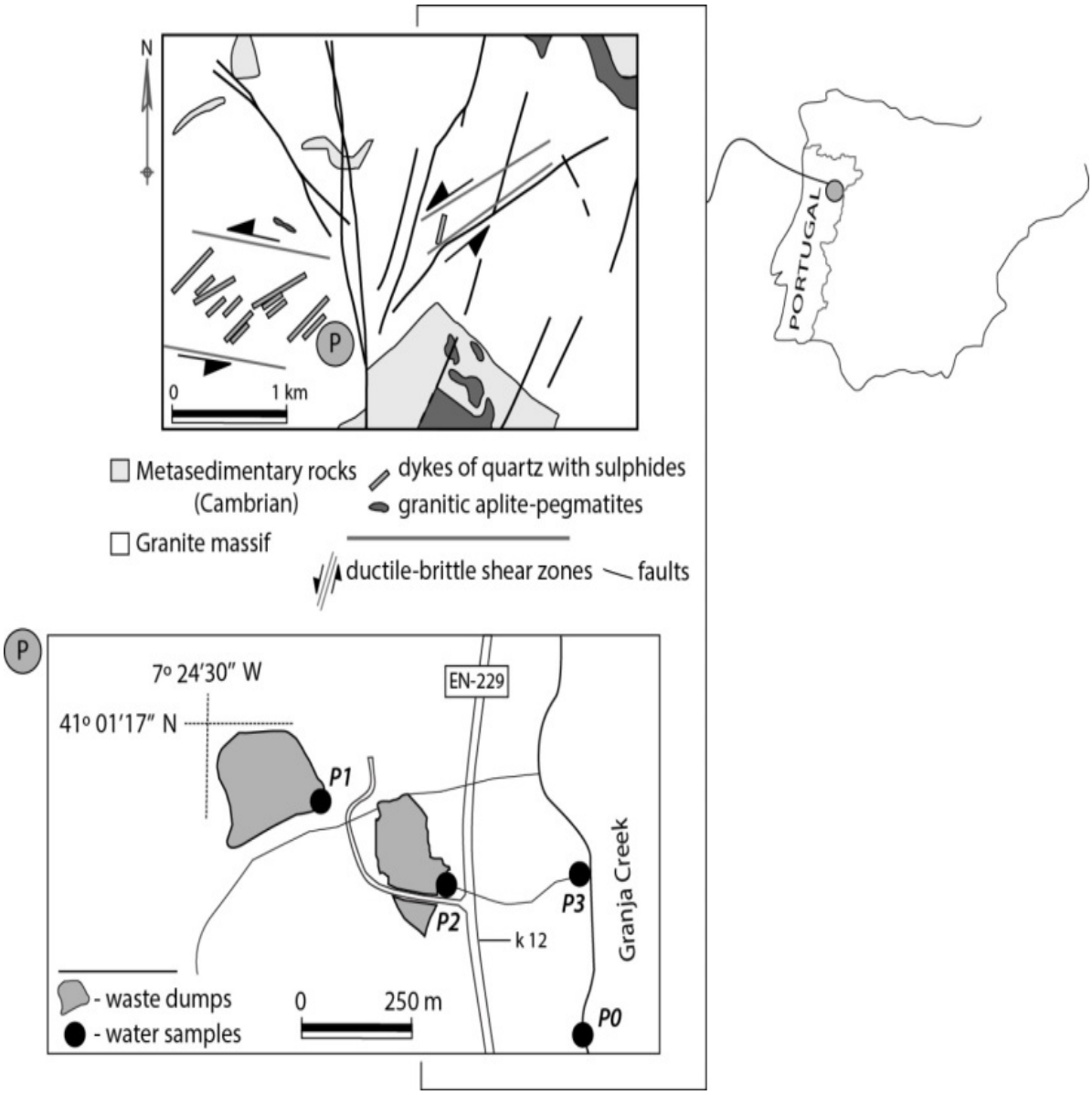

Figure 1 *Penedono mine with simplified geology, sketch of the waste dumps and water sampling sites*

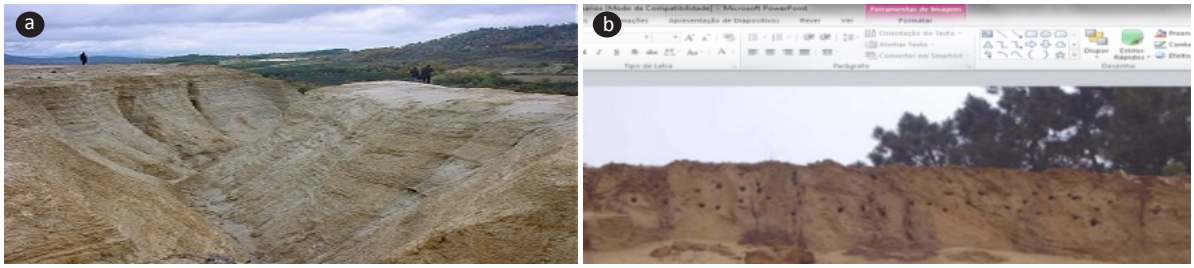

Figure 2 Panoramic image evidencing the steepness and ravine (a) and slope encrustation with surface hardpans at the base (b)

site P0, upstream the influence of the mine. The pH, electric conductivity (EC), and redox potential (Eh) were measured in the field with multiparameter model Orion 5. The samples were stored in pre-washed polyethylene bottles and refrigerated (<4°C). They were analysed for total acidity and sulfate. Metals and arsenic were analysed by inductively coupled plasma mass spectrometry (ICP-MS) in filtered and acidified aliquot until pH < 2.

Blanks, replicates and stock solutions were used to assess quality control of the results. The accuracy of the methods was verified using certified patterns. The measurement precision was within relative standard deviation (RSD) of 5% for all methods.

Results and discussion

AMD properties

Table 1 shows the properties of the surface water. The low pH (3-4) indicates typical conditions of AMD. The sulfate nature is demonstrated by comparison with the background (P0). Also, such a comparison indicates the influence of the waste dumps, generating high contents of metals and arsenic.

Secondary minerals and aggregates

The new minerals are over and mixed with fine grains of quartz and muscovite. Consequently separation for obtaining pure samples is a rather difficult task. Table 2 presents a list of the identified phases, with respective distribution. An estimation of abundance is also provided. Field images in figure 3a-c illustrate habits and occurrence modes of some sulfates, including the relatively uncommon metavoltine, but highly expressive in these waste dumps. It is rare to observe single phases or pure aggregates; generally the sulfates form assemblages more or less complex as shown in the SEM images (Figure 3 d-g).

Hydrous sulfates are distributed throughout the area of the waste dumps. However, the highest abundance and diversity were observed on the exposed slopes, in condition of high evaporation, which leads to salt efflorescences. Also, downstream of the waste dumps, there are abundant gypsum and pickeringite, filling fractures in the margins of the small receiving creek (Figure 1). The group of minerals with the general form $M^{2+}Al_2(SO_4)_3\ 22H_2O$ occurs abundantly, though sometimes it is difficult to assure their refinement. The extremes pickeringite (Mg) and halotrichite (Fe) are the most commonly discriminated. In terms of iron hydrous sulfates, Fe precipitates in different oxidation states, including abundant melanterite, copiapite, and rhomboclase. They are profuse at the base and at middle height of the exposed slopes, mixed and over the fine grained tails.

Table 1 Water properties of AMD and surface background.

Sampling site	pH	EC	Eh	SO_4	Al	Fe	Mn	Zn	As
		(µS/cm)	(mV)			mg/L			
P3-P1 (n=6)	3.5	1196	486	486	36.57	23.36	16.85	2.24	2.54
	2.8-3.6	971-1506	456-526	511-652	19.0-52.6	1.40-42.2	7.01-28.2	2.08-2.41	0.028-7.54
P0 (n=2)	6,3	69	240	5.1	2.3	0.290	0.650	0.012	0.00053

Table 2 Secondary phases associated with sulphide-rich wastes in Penedono; + rare; +++++ very abundant

Mineral	Ideal formula	Abundance	Distribution
Melanterite	FeSO4·7H2O	++++	Exposed slopes
Rozenite	FeSO4·4H2O	+++	
Szomolnokite	FeSO4·H2O	+	
Copiapite	Fe2+Fe43+(SO4)6(OH)2 20H2O	+++	
Rhomboclase	HFe3+(SO4)2 4H2O	+	
Epsomite	MgSO4·7H2O	+	
Starkeyte	MgSO4·4H2O	++	
Halotrichite	FeAl2(SO4)4·22H2O	++++	Exposed slopes and creek margins
Pickeringite	MgAl2(SO4)4·22H2O	++++	
Wupatkiite	(Co, Mg, Ni) Al2(SO4)4·22H2O	++	
Apjohnite	MnAl2(SO4)4·22H2O	++	
Alunogen	Al2(SO4)3·17H2O	++++	Exposed slopes
Tamarugite	NaAl(SO4)2 6H2O	+++	
Kalinite	KAl(SO4)2 11H2O	+	
Chalcanthite	CuSO4·7H2O	+	
Metavoltine	K2Na6Fe2+Fe3+6O2(SO4)12·18H2O	++++	
Gypsum	CaSO4 2H20	+++++	ubiquitous
Scorodite	FeAsO4 2H2O	+++++	
Jarosite	KFe3 (SO4)2(OH)6	+++++	
Goethite	FeOOH	+++	Widespread in hardpans
Schwertmannite	Fe8 O8(SO4)(OH)6	+	Water emergence
Amorphous	Fe arsenate and Fe oxyhydroxide	++++	Widespread

Most of the soluble minerals have been documented in AMD-systems worldwide, like melanterite and copiapite (e.g. Valente et al., 2015; Sánchez-España 2008; Durães et al. 2008). Nevertheless, some less common phases were identified, such as metavoltine. Schwertmannite, usually abundant, was only detected at the base of the waste dump, around P1 (Figure 1). On the contrary, jarosite is ubiquitous. The first was observed at the base, where pH rounds 3.0, which is in accordance with equilibrium conditions for this mineral (Bigham et al., 1994). Lower values are expected in the pore water of the waste dumps, favoring the precipitation of jarosite as noted by the model of evolution of secondary Fe minerals proposed by several authors (e.g Bigham et al., 1994; Montero et al. 2005). Together with jarosite, scorodite is widespread. As observed by Murciego et al. (2011), these are the two main products of arsenopyrite oxidation. Jarosite occurs as powder masses in dry channels or in crustified aggregates. The same occurs with scorodite, which appears as bluish or greenish powder, plates, and crustified structures, which configure hardpans. Hardpans are aggregates of primary and secondary minerals, in which a cementing material progressively assures the agglutination. Formation of hardpans in sulphide-rich environments has been documented by several authors (e.g. Lottermoser and Ashley 2006; Courtin-nomade et al., 2003). The entire base of the Penedono waste dumps is surrounded by hard and sometimes large crusts (hardpans) of different nature. They enclose grains of inherited phases like quartz, muscovite, feldspars, and sulphides, cemented mainly by an AMD-precipitate that assures cohesion.

Figure 4 illustrates the main types of hardpans, which are mostly Fe-rich and As-rich crusts. In addition to jarosite and scorodite, encrusting cements were found to include clay minerals and amorphous material. Valente et al. (2015) documented the nature of the non-crystalline nanoprecipitates, comprising iron oxyhydroxides and iron arsenates.

Hardpans show varied colors, hardness, and cohesion. The Fe-rich hardpans are cemented by major jarosite often in coexistence with goethite (Figure 4a-b). They form the most cohesive and can appear massive or, more usually, as banded structures with yellow-orange-reddish thin

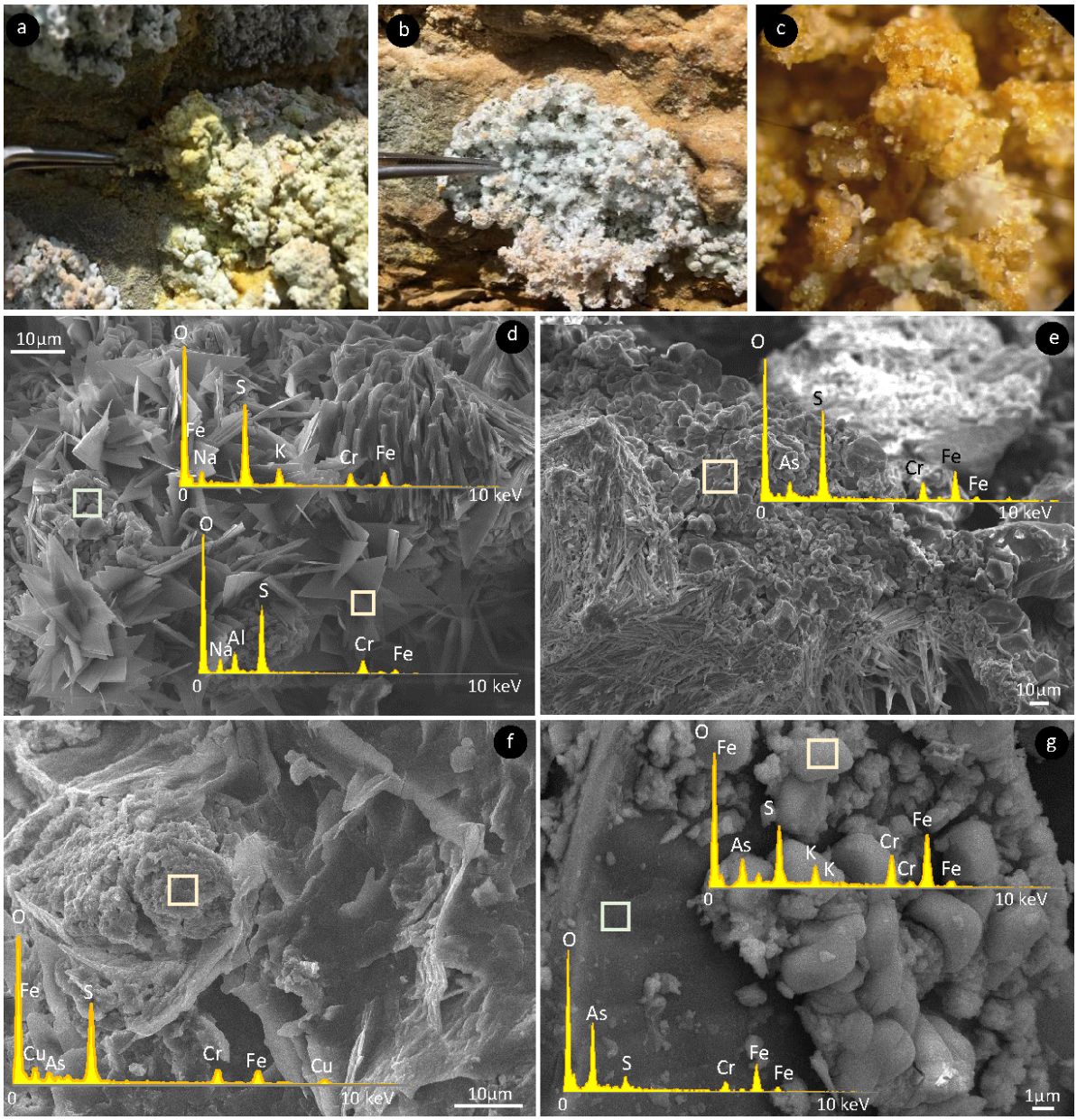

Figure 3 *Salt efflorescences and typical assemblages. a) yellow-greenish botryoidal copiapite in association with a mixture of Al- sulfates; b) Radiated aggregates of acicular minerals of the group pickeringite- Wupatkiite-Apjohnite; c) Yellowish brown crystals of metavoltine; d) SEM images and EDS spectra of platy tamarugite enclosing aggregates of jarosite and tabular copiapite; e) Acicular halotrichite and melanterite (probably adsorption of As); f) Platy alunogen enclosing aggregates of chalchantite; g) Jarosite over a plate of scorodite*

layers. Sometimes, the layers indicate the flow direction at the moment of the tailings deposition as illustrated in figure 4-c. Also, there are whitish fragile hardpans, in which kaolinite is the major cementing material (Figure 4-d). The As-rich hardpans, encrusted by the iron arsenate, assume blue or blue-greenish colors (Figure 4 e-f). Though there are these two extremes (Fe and As), hardpans incorporate intermediate proportions of jarosite, goethite, scorodite and amorphous materials.

Neutralization, precipitation and adsorption are important attenuation processes in the presence of mining wastes (Hammarstrom et al., 2005; Wilkin, 2007). Precipitation of evaporative minerals avoid, although temporarily, release of metals and acidity. On the other hand, jarosite and scorodite are more stable in acid conditions, thus they should be more effective in retention of contaminants. For example, DeSisto et al. (2011) emphasize this role of scorodite due to its relatively low solubility (<1 mg/L at pH

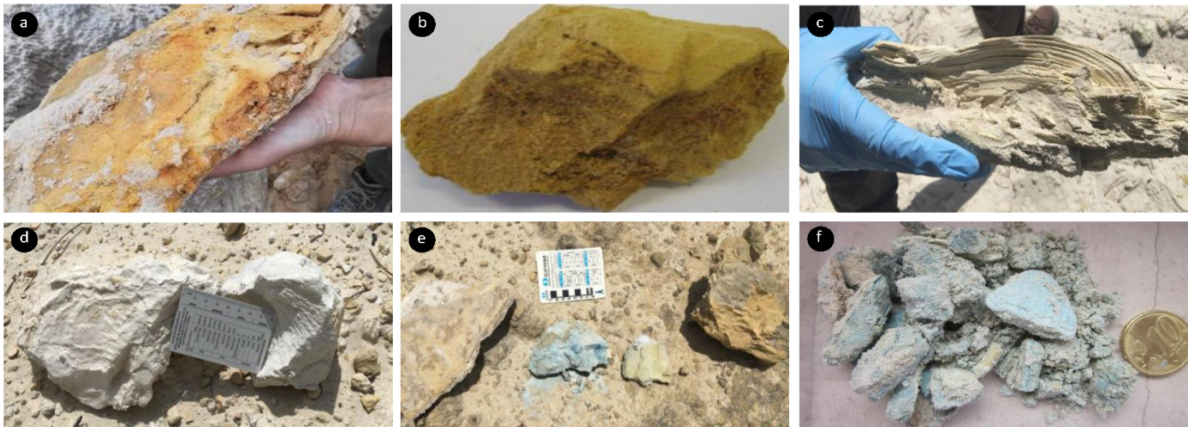

Figure 4 Typical hardpan. a) Banded Fe-rich hardpan cemented by jarosite and goethite; b) Fe-rich hardpan mainly composed by massive jarosite; c) and d) fragile hardpans, mainly cemented by kaolinite; e) and f) Light blue As-rich hardpans

3–4) and high contents of As (43–52% As_2O_5). Therefore, by stability of the cement and also the hardness, Fe and As-rich hardpans should be the more efficient supergenic structures limiting the oxidative dissolution of sulphides and, consequently, the mobility of PTE.

Conclusion

The inventory of secondary minerals indicated a considerable number of phases, mostly of Fe and Al, which are typical of AMD systems. In their composition and on their surfaces the sulfates contain PTE. Most of them are soluble and therefore with a limited efficiency controlling mobility of metals and As. However, there is a profusion of minerals relatively more stable, like jarosite and scorodite. Furthermore, both may act as cementing material, forming hardpans. Field observations, confirmed by the mineralogical study, indicate the high abundance and the environmental relevance of hardpans. They act as barriers to oxidation and dissolution of reactive phases, thereby inhibiting the mobility of PTE.

Acknowledgements

This work was co-funded by the European Union through the European Regional Development Fund, based on COMPETE 2020 - project ICT (UID/GEO/04683/2013) with reference POCI-01-0145-FEDER-007690 and project Nano-MINENV number 029259. The authors are grateful to the suggestions of the reviewers.

References

Abreu M.; Matias M.J.; Magalhães M.F.; Basto M.J. (2007) Potencialites of Pinus pinaster and Cytisus multiflorus on the phytostabilization of the Santo Antonio (Penedono) gold mine dumps. Revista de Ciências Agrárias, 30(2), 335-349.

Bigham JM, Carlson L, Murad E. (1994) Schwertmannite, a new iron oxyhydroxy-sulphate from Pyhasalmi, Finland, and other localities. Mineral Mag 1994;58:641–8.

Courtin-nomade A, Bril H, Neel C, Lenain JF (2003) Arsenic in iron cements developed within tailings of a former metalliferous mine—Enguialès, Aveyron, France, Applied Geochemistry, 18(3):395-408, DOI 10.1016/S0883-2927(02)00098-7

DeSisto S, Jamieson HE, Parsons MB (2011) Influence of hardpan layers on arsenic mobility in historical gold mine tailings, Applied Geochemistry 26, 2004–2018, doi:10.1016/j.apgeochem.2011.06.030

Dold B (2014) Evolution of Acid Mine Drainage Formation in Sulphidic Mine Tailings, Review, Minerals, 4, 621-641; doi:10.3390/min4030621.

Durães N, Bobos L. Eduardo Ferreira da Silva E (2008) Simple efflorescent sulphates from Iberian Pyrite Belt (Portugal), Macla 10, 126-128

Gomes P, Valente T, Pamplona J, Sequeira Braga MA, Pissarra J, Grande JA, 2014. Metal uptake by native plants and revegetation potential of mining sulfide-rich waste-dumps. International Journal of Phytoremediation, 16(7-12),1087-103. https://doi.org/10.1080/15226514.2013.810586

Hammarstrom, J.M., Seal II, R.R., Meier, A.L., Kornfeld, J.M. (2005) Secondary sulfate minerals associated with acid drainage in the eastern US: recycling of metals and acidity in surficial environments. Chem. Geol. 215: 407–431.

Lottermoser B, Ashley P (2006) Mobility and retention of trace elements in hardpan-cemented cassiterite tailings, north Queensland, Australia, Environ Geol, 50: 835–846 DOI 10.1007/s00254-006-0255-8

Montero C; Brimhall GH; Alpers, CN; Swayze GA (2005) Characterization of waste rock associated with acid drainage at the Penn Mine, California, by ground-based visible to short-wave infrared reflectance spectroscopy assisted by digital mapping, USGS Staff, Published Research. 491.

Murciego A, Álvarez-Ayuso E, Pellitero E, Rodríguez MA, García-Sánchez A, Tamayo A, Rubio J, Rubio F, Rubin J (2011) Study of arsenopyrite weathering products in mine wastes from abandoned tungsten and tin exploitations, Journal of Hazardous Materials 186 (2011) 590–601, doi:10.1016/j.jhazmat.2010.11.033

Olías M, Nieto JM (2015) Background Conditions and Mining Pollution throughout History in the Río Tinto (SW Spain), Environments, 2, 295–316; doi:10.3390/environments2030295

Sánchez España J (2008) Acid Mine Drainage in the Iberian Pyrite Belt: an Overview with Special Emphasis on Generation Mechanisms, Aqueous Composition and Associated Mineral Phases, Macla 10, 34-43

Valente T, Grande JA, de la Torre ML, Santisteban M, Cerón JC (2013) Mineralogy and environmental relevance of AMD-precipitates from the Tharsis mines, Iberian Pyrite Belt (SW, Spain), Applied Geochemistry 39 (2013) 11–25, doi.org/10.1016/j.apgeochem.2013.09.014

Valente T, Gomes P, Sequeira Braga MA, Dionisio A, Pamplona J, Grande JA (2015) Iron and arsenic-rich nanoprecipitates associated to clay minerals in sulfide-rich waste dumps. Catena, 131, 1-13. DOI: 10.1016/j.catena.2015.03.009.

Wilkin T (2007) Metal attenuation processes at mining sites. U.S. Environmental Protection Agency, Washington, DC, EPA/600/R-07/092, 2007.